Downloaded from rsta.royalsocietypublishing.org

PHILOSOPHICAL TRANSACTIONS OF THE ROYAL SOCIETY A MATHEMATICAL, PHYSICAL & ENGINEERING SCIENCES

Studies in Hydrodynamic Thrust Bearings. III. The Parallel Surface Bearing

C. L. Robinson and A. Cameron

Phil. Trans. R. Soc. Lond. A 1975 **278**, 385-395
doi: 10.1098/rsta.1975.0031

Email alerting service

Receive free email alerts when new articles cite this article - sign up in the box at the top right-hand corner of the article or click **here**

To subscribe to *Phil. Trans. R. Soc. Lond. A* go to: **http://rsta.royalsocietypublishing.org/subscriptions**

This journal is © 1975 The Royal Society

Downloaded from rsta.royalsocietypublishing.org

Phil. Trans. R. Soc. Lond. A. **278**, 385–395 (1975) [385]
Printed in Great Britain

STUDIES IN HYDRODYNAMIC THRUST BEARINGS

III. THE PARALLEL SURFACE BEARING

By C. L. Robinson and A. Cameron
Lubrication Laboratory, Department of Mechanical Engineering, Imperial College of Science and Technology, London S.W. 7

(*Communicated by H. Ford, F.R.S. – Received* 23 *April* 1974)

[Plate 16]

CONTENTS

The parallel surface bearing is interesting in that on first sight it completely contradicts the classical Reynolds lubrication theory. Secondly its mode of operation has only recently been capable of detailed explanation.

The optical technique, described in the last section offered a precise method of proving that thermal distortion of the pads provides the necessary converging wedge.

When the experimental results were analysed by the theory developed in part I, it was seen that thermal distortion does in fact, explain them very accurately. The simplifying assumptions needed to solve the Reynolds and energy equations are somewhat stretched, but, within this limitation, the agreement between the proposed mechanism and the theory is good.

The Royal Society is collaborating with JSTOR to digitize, preserve, and extend access to *Philosophical Transactions of the Royal Society of London. Series A, Mathematical and Physical Sciences.* www.jstor.org

Downloaded from rsta.royalsocietypublishing.org

Nomenclature

B	pad width	U	mean sliding speed
h_0	minimum film thickness	δ	distortion
k	thermal conductivity of pad	η	average film viscosity
p_s	specific load	ρ	lubricant density
t	pad thickness	σ	lubricant specific heat

Introduction

In the preceding two parts the theoretical evaluation of thrust bearing distortions and their measurement by interferometry has been described. In this part these methods are applied to parallel surface bearings, a configuration of considerable interest. Their interest first is intrinsic, in that they act by reason of temperature effects which, therefore, require the rather advanced analysis developed earlier for their treatment.

In 1876 a committee of the Institution of Mechanical Engineers, which included Lord Rayleigh, sponsored some work on journal bearings by Beauchamp Tower. The two reports were analysed by Stokes and by Reynolds, whose 1886 paper laid the foundations of hydrodynamic lubrication. Tower extended the work to footstep bearings which used surfaces manufactured to be flat and parallel. One surface had radial grooves in it. These reports were published in 1888 and 1891. A reproduction of the grooved plate thrust apparatus is given by Cameron (1966), together with detailed references.

In these reports no mention whatsoever is made of Reynolds's paper and that these parallel surfaces (which carried an appreciable load on a fluid film) apparently contradict Reynolds's theory. Nor did the academics make any mention of the contradictory nature of Tower's findings. One can only speculate that Tower did not wish to embarrass the hydrodynamicists who (on their side) were perhaps willing enough to disregard a most awkward finding.

At all events this work was completely forgotten.

Fogg in 1946 rediscovered the parallel surface thrust bearing and appropriately read a paper to the Institution of Mechanical Engineers who had sponsored the original work 60 years earlier. He suggested that the load was carried by the oil heating up and expanding during its passage through the bearing thus causing a 'thermal wedge'.

In the discussion Swift doubted whether this mechanism would suffice and suggested thermal distortion as a more likely cause. This was printed with the discussion of another paper and was consequently lost for a further 15 years.

Fogg's suggestion was analysed by Cameron & Wood (1946), Osterle, Charnes & Saibel (1953) who showed that it was not 'powerful' enough to provide the observed load carrying capacity. The idea of the thermal distortion of the moving surfaces was then proposed by Cameron (1960) and by Dowson & Hudson (1963), ignorant that Swift had, in fact, suggested it in 1946.

A number of papers were published showing that thermal distortion was the most probable mode of operation of the bearing. Neal (1963), Ettles & Cameron (1963) and Hemingway (1965) all contributed to the analysis.

Having used interferometry for tilting pads it seemed that this technique was the correct way of proving the importance of thermal distortion, as it could be followed visually during the progress of the test.

This part of the work describes how such experiments were undertaken.

Downloaded from rsta.royalsocietypublishing.org

Apparatus

The test machine was exactly as described in part II with the exception of the bearing. This was an annulus 76 mm in diameter of EN58 stainless steel with six deep radial grooves in it such that the six sectors were connected only by thin strips of metal (figure 1). The bearing was supported by six wide radial supports, each of angular width one-third of the pad. The pad and support centres were coincident. The complete annulus was flat to within three light fringes (0.81 μm) and any one pad was better than ½ fringe (0.14 μm).

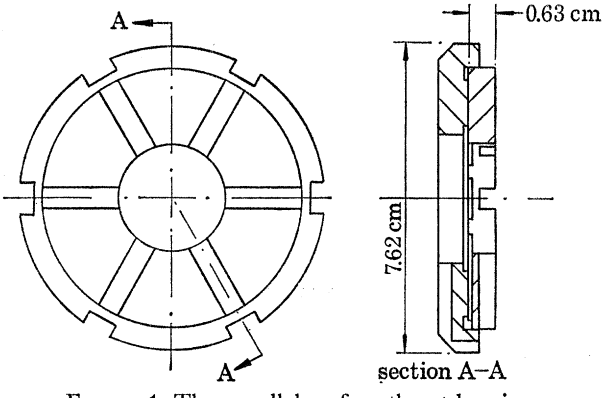

Figure 1. The parallel surface thrust bearing.

Even greater difficulty was found in preventing scratching with these pads than with the tilting ones. A typical interferogram is shown in figure 2, plate 16, with the digital print out plot superposed. It is important to note that though the pad is scratched over an appreciable portion, the information available from the interference fringes is not seriously reduced. The contour print out plot shows the continuity of the fringes and the absence of fringes over the damaged area had little effect on the data. The reason being that the scratching was *surface* damage, reducing the *reflectivity*, but hardly influencing the film shape.

Test procedure

The procedure used for the tilting pad bearing tests was followed exactly. Approximately twice the load was needed to obtain the same specific loading, as there were six pads instead of three. The power absorbed was larger so the maximum speed was reduced, limited by motor power.

Specific loads of 1.37, 2.76, 4.14 and 5.52 MN/m² were tested at nominal speeds of 209, 419, and 576 rad/s. The 5.52 MN/m², 209 rad/s test was omitted for fear of scuffing.

Results

The results of this study will be presented in the same form as was used in part II. First the interferograms, processed to give 0.51 μm contours, are presented, to give an overall view of the film shape. The very important minimum film thickness is analysed, then the pressure distribution, the film temperature leading to the heat balance and the distortion of the pads. Finally the technique of the theoretical analysis which relies entirely on the thermal distortion for the load carrying capacity is considered, with a discussion of the film shape and effect of distortion. The theoretical 0.51 μm film contours are given alongside the experimental findings in the beginning, the long cycle to find them being the subject of the theoretical section.

Downloaded from rsta.royalsocietypublishing.org

The results section ends with a comparison of tilting and parallel pad operation. Surprisingly the differences are not as large as one might imagine considering the way the film is formed.

Film thickness contours

The reduction of data from the interferograms to numerical form and hence to a digital contour print out was described in part II. Typical results are shown in figure 3. Successive contours are drawn at 0.51 μm intervals.

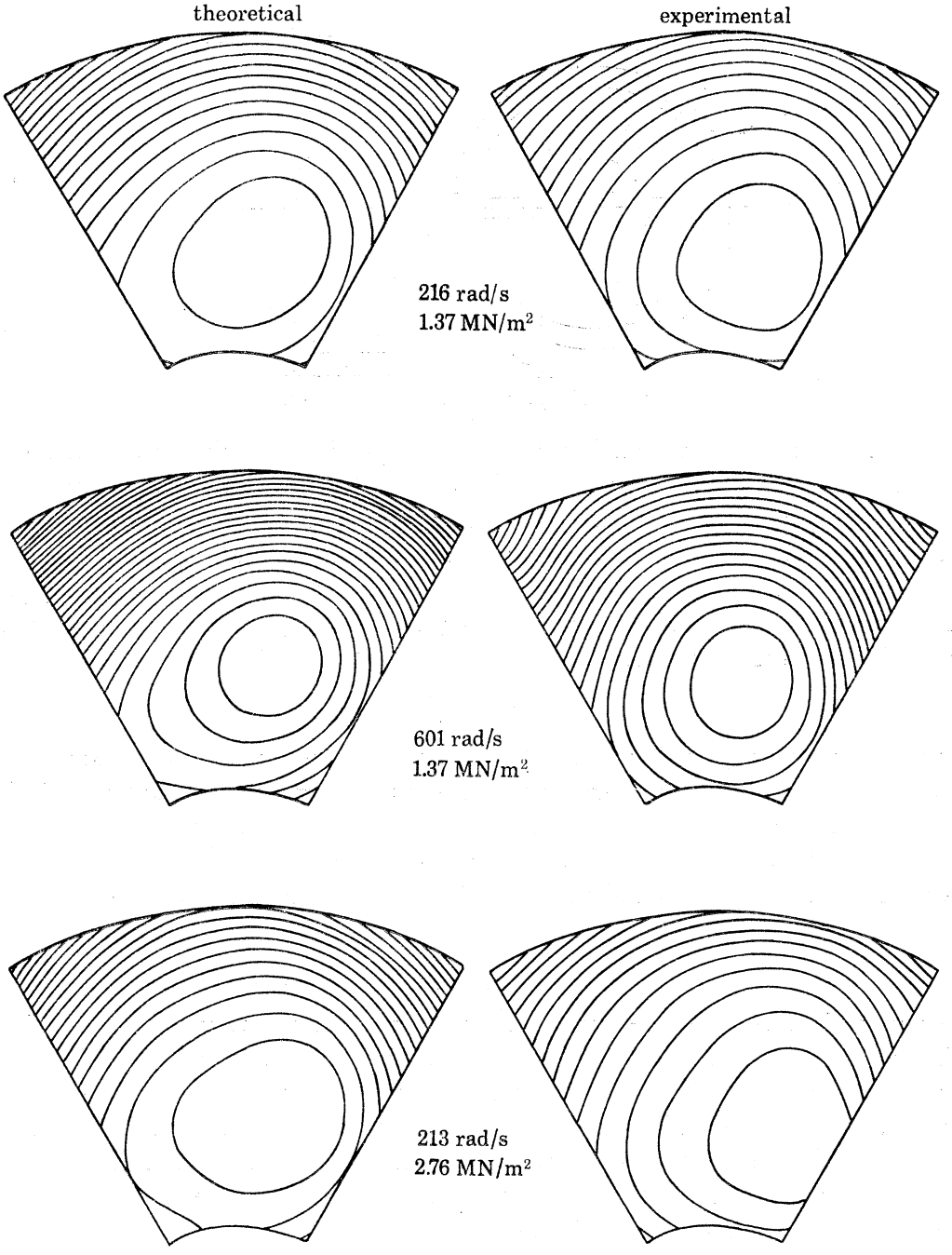

FIGURE 3. For description see opposite.

PHILOSOPHICAL TRANSACTIONS OF THE ROYAL SOCIETY A MATHEMATICAL, PHYSICAL & ENGINEERING SCIENCES
PHILOSOPHICAL TRANSACTIONS OF THE ROYAL SOCIETY A MATHEMATICAL, PHYSICAL & ENGINEERING SCIENCES

Downloaded from rsta.royalsocietypublishing.org

The minimum film thickness is now closer to the middle than to the trailing edge and nearer the inner radius. The higher the speed and the lower the load the nearer the minimum gets to the centre. The total distortion increases with speed but is insensitive to load. When the distortion increases markedly there is a larger divergent section and here lubricant rupture occurs. This is shown in figure 4, plate 16, with a speed of 582 rad/s and load of 2.76 MN/m². In the cavitation 'fingers' there are $1\frac{1}{2}$ times more fringes than outside, which is the ratio of the refractive index of oil/vacuum or air. This strongly suggests that the fingers are air (or vapour) filled.

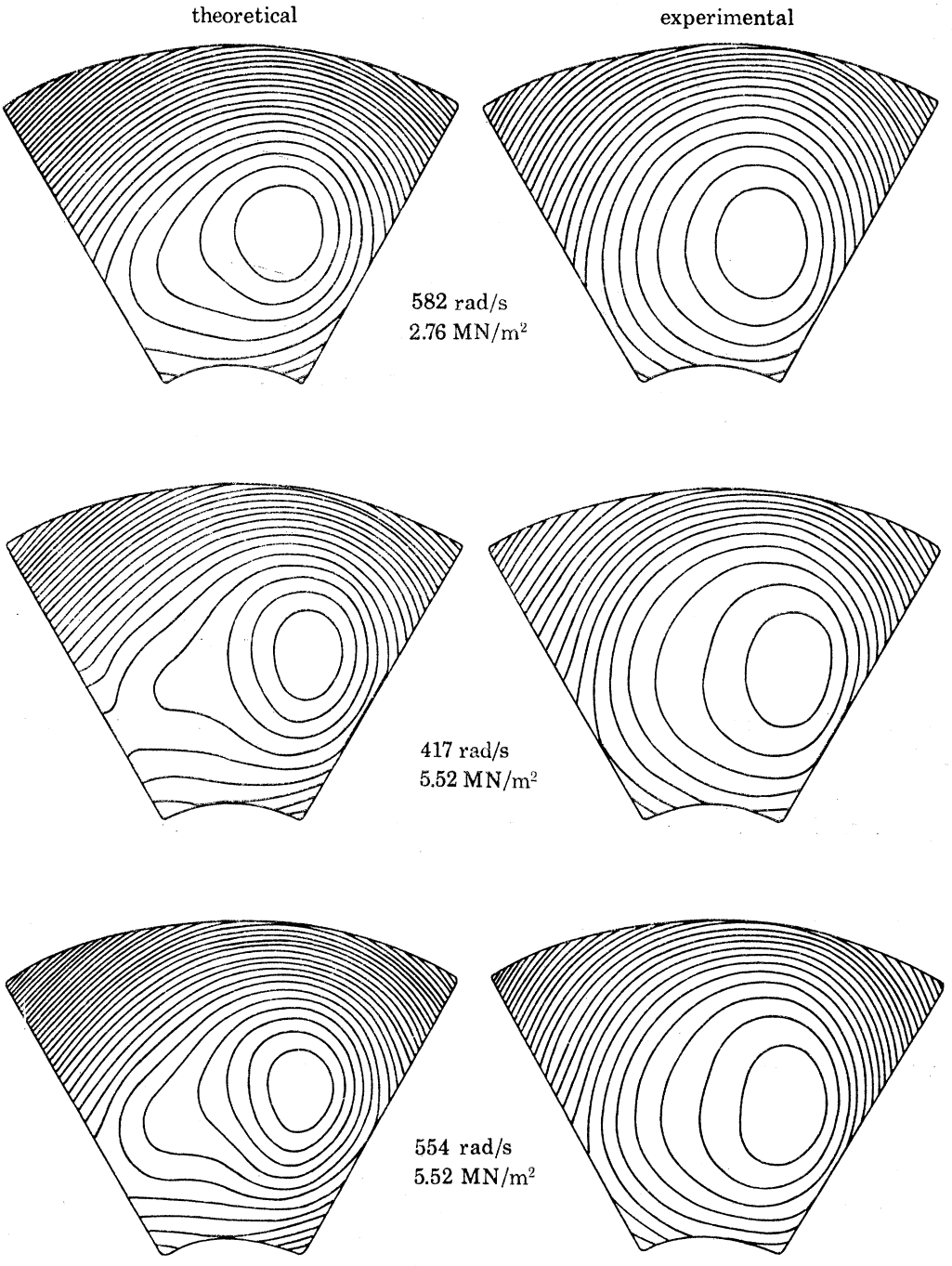

FIGURE 3 (*continued*). Comparison of experimental and theoretical film shapes, 0.51 μm contours.

PHILOSOPHICAL TRANSACTIONS OF THE ROYAL SOCIETY A MATHEMATICAL, PHYSICAL & ENGINEERING SCIENCES
PHILOSOPHICAL TRANSACTIONS OF THE ROYAL SOCIETY A MATHEMATICAL, PHYSICAL & ENGINEERING SCIENCES

Downloaded from rsta.royalsocietypublishing.org

Minimum film thickness

The minimum film thickness, temperature and pressure distribution were all calculated from the measured film shapes and temperatures using the hydrodynamic programme described in part I. When negative pressures in the diverging part were predicted by the Reynolds equation they were put equal to zero. This has been shown to give the correct boundary conditions by Osborne (1966).

Minimum film thicknesses calculated *ab initio* and from the measured film shape are shown in figure 5.

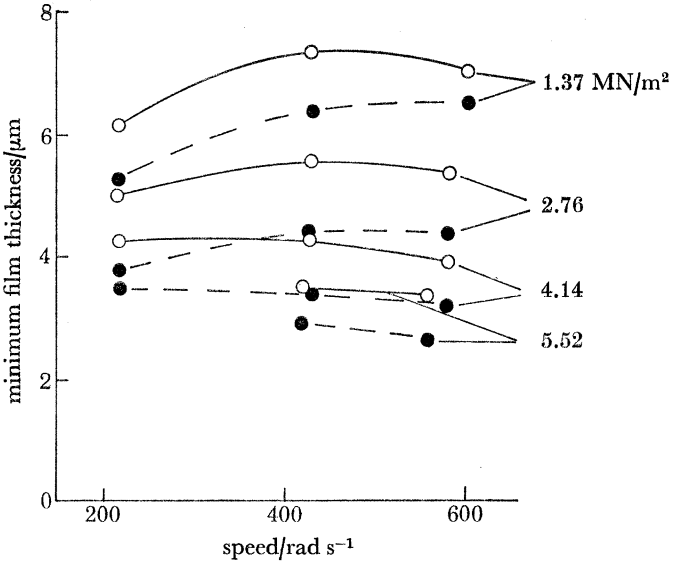

FIGURE 5. Minimum film thickness both fully calculated and from measured film shape. ○, Calculated values based on measured film shape; ●, calculated values based on predicted film shape.

At low loads there is an optimum speed of 472 rad/s. At high load film thickness falls uniformly. This is due to

(1) a reduction in effective viscosity with speed, and

(2) to a loss of effective area due to cavitation towards the trailing edge.

Pressure distribution

The calculated pressure distribution is shown for 1.37 MN/m² and speeds of 216, 427, and 601 rad/s and 5.52 MN/m² and 554 rad/s in figure 6. The general shape is the same, but the cavitated area *decreases* as the load goes up and speed down.

The centre of pressure is well towards the trailing edge, but always less than $\frac{1}{6}$ pad width from the centre circumferentially and never more than 2 % away from the centre radially.

Film temperature

The measured inlet temperatures and bulk temperature were higher than the tilting pad case due to greater churning and friction. The predicted values of outlet temperature, based on measured film shape agreed well with experiment (4 K being the maximum error) as did theoretical and measured temperatures. Typical results are shown in figure 7. The maximum

Downloaded from rsta.royalsocietypublishing.org

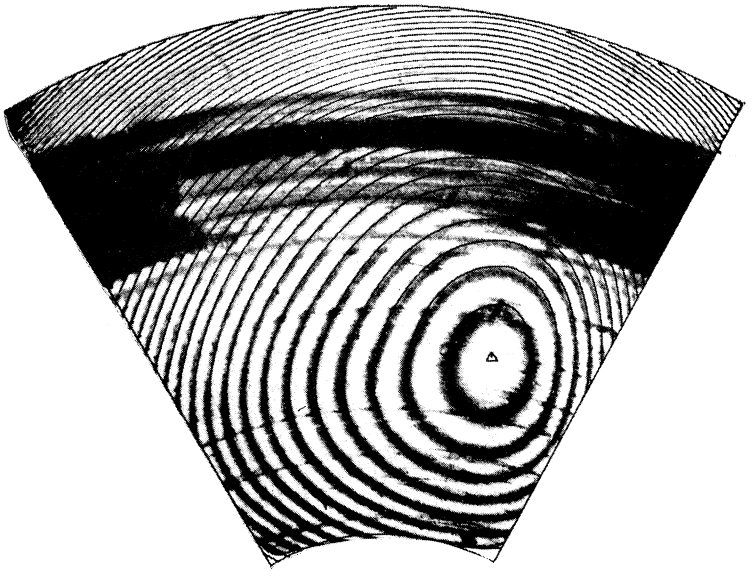

FIGURE 2. Typical interferogram with digital print out superimposed.

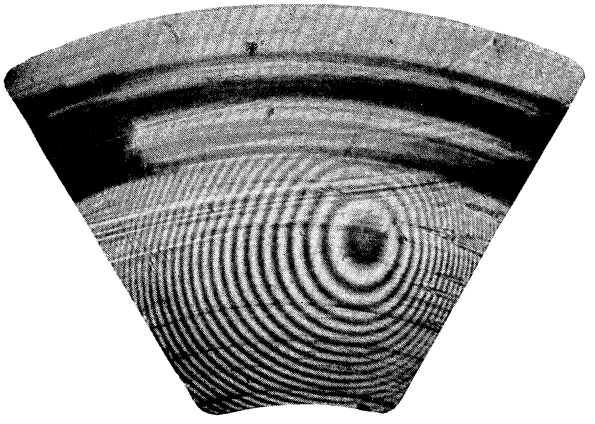

FIGURE 4. Interferogram of pad load 2.76 M/Nm², speed 582 rad/s showing film rupture.

(*Facing p.* 390)

PHILOSOPHICAL TRANSACTIONS OF THE ROYAL SOCIETY A MATHEMATICAL, PHYSICAL & ENGINEERING SCIENCES

PHILOSOPHICAL TRANSACTIONS OF THE ROYAL SOCIETY A MATHEMATICAL, PHYSICAL & ENGINEERING SCIENCES

Downloaded from rsta.royalsocietypublishing.org

temperature is well before the outlet. This has been noted in earlier papers (Neal 1963; Ettles & Cameron 1966).

The temperature along the inlet boundary was found not to be constant, due probably to hot oil carryover.

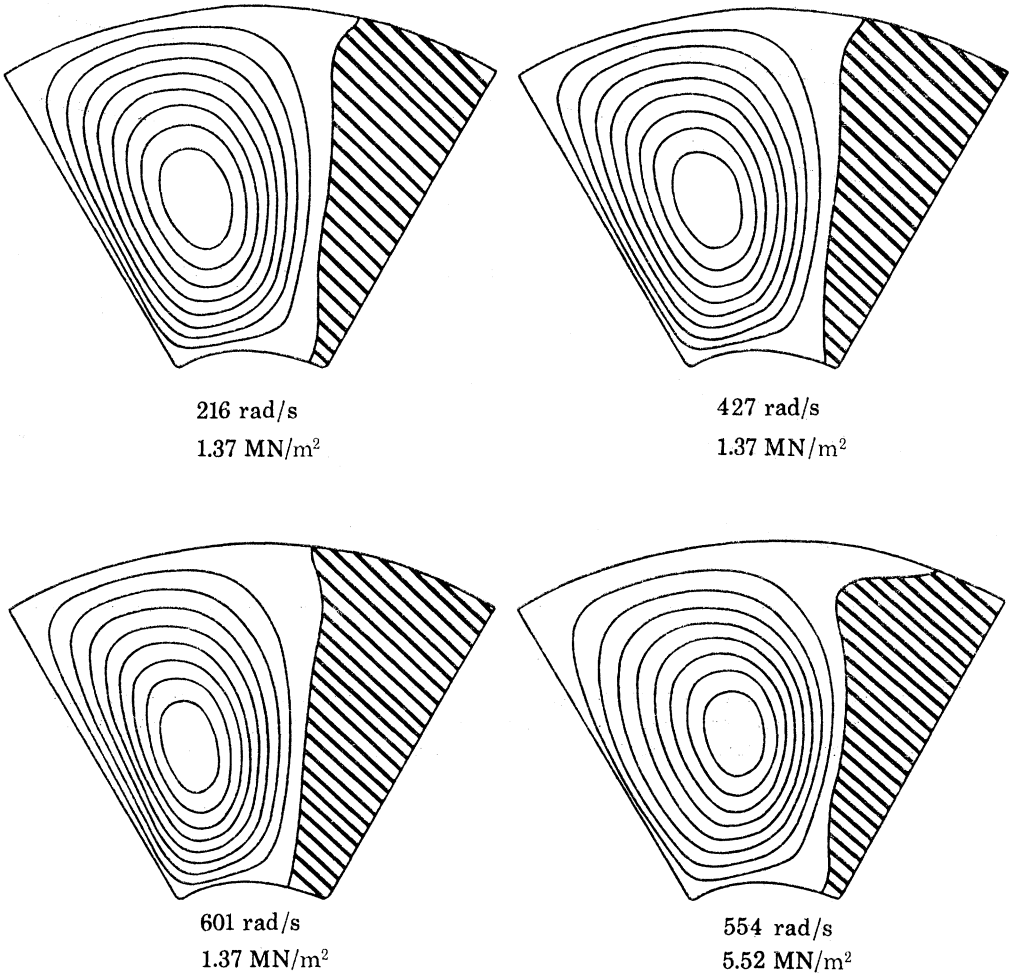

FIGURE 6. Pressure distribution, showing effects of speed and load on cavitated region.

Heat balance

The ratio of convected to conducted heat is shown in figure 8 plotted against the parameter

$$\frac{\sigma\rho}{k}\frac{Uh_0 t}{B}.$$

A greater proportion of the heat is conducted away than for tilting pads due to the better heat flow path in the fixed pad design.

Distortion

Longitudinal and transverse distortions (defined in figure 15 of part II) which cause the oil film to be formed, are shown in figure 9 for loads of 1.37–5.52 MN/m² and at two speeds 209 and 576 rad/s. They do not differ greatly in form from those presented for tilting pads but are about double in magnitude. There is also a general increase with speed, longitudinal distortion reduces with load, transverse unaffected.

Downloaded from rsta.royalsocietypublishing.org

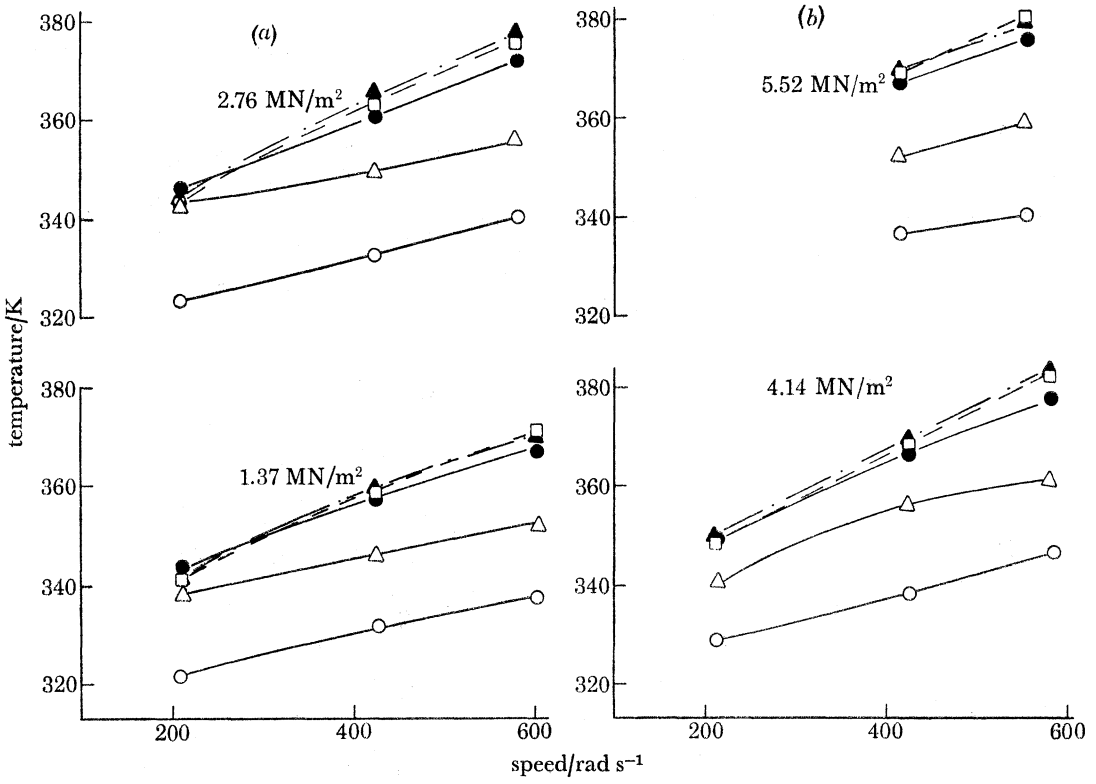

FIGURE 7. Theoretical and measured temperatures. ○, Bulk oil temperature; △, average inlet temperature; ●, average outlet temperature, measured; □, average outlet temperature, calculated, based on measured film shape; ▲, average outlet temperature, measured, based on predicted film shape.

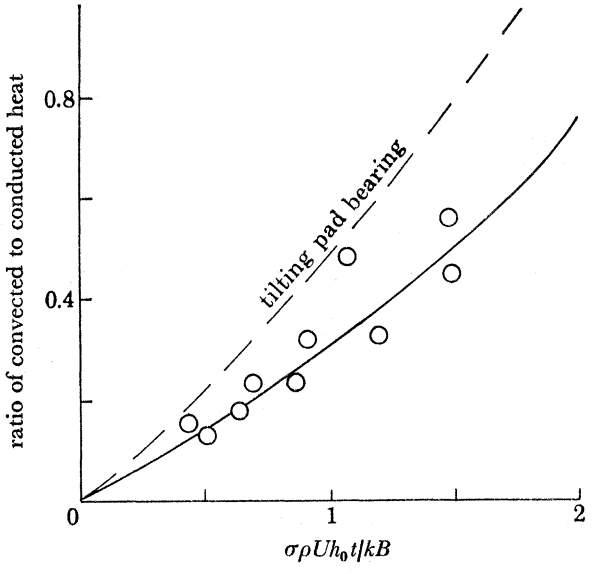

FIGURE 8. Ratio of convected to conducted heat plotted against $(\sigma\rho/k)$ (Uh_0t/B).

Downloaded from rsta.royalsocietypublishing.org

Theoretical analysis

In all this work it was found pressure bending of the pad could be neglected. This is because first the support occupies one-third of the pad circumferential width. The unsupported cantilever length is, therefore, only two-thirds of the tilting pad and as bending deflexion varies as length cubed, it is 70 % less. Secondly, the web joining the pads reduces the deflexion further. Thirdly, in the tilting pad, bending was a minor constituent so here it is even less, compared with thermal distortion, as since for a given load and speed the temperature difference across the pad thickness is nearly double.

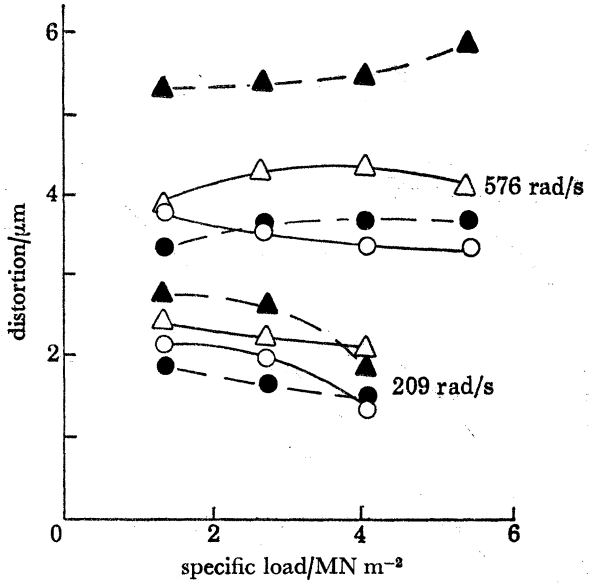

Figure 9. Plot of longitudinal and transverse distortion against load for speeds of 209 and 576 rad/s. ○, Longitudinal, measured; ●, longitudinal, calculated; △, transverse, measured; ▲, transverse, calculated.

The agreement between theory and measurement can only be described as fair. The longitudinal distortion (figure 9) is 20 % in error, while the transverse distortion can be as much as 40 % too high for the highest speed and load.

The various contributions to the total distortions are listed in table 1. A negative sign indicates a concave movement. As expected thermal distortion assumes the dominant role for the parallel surface bearing with direct compression contributing to a large extent at high loads.

Table 1. Contribution of various distortion modes

		longitudinal distortion/μm					
		thermal bending		pressure bending		direct	
speed rad/s	specific load MN/m²	pad	collar	pad	collar	thermal expansion	direct compression
281	1.37	1.412	1.050		−0.069	−0.104	−0.514
600	1.37	1.787	1.952		−0.066	−0.107	−0.590
213	2.76	1.767	1.182	neglected	−0.147	−0.108	−0.899
582	2.76	2.187	2.066		−0.147	−0.124	−1.120
416	5.52	2.062	1.878		−0.310	−0.081	−2.014
554	5.52	2.680	2.237		−0.315	−0.141	−2.232

Downloaded from rsta.royalsocietypublishing.org

Discussion of calculated and measured film shapes

The calculated film shapes were in fact presented with those measured in figure 3. They are in good agreement, the predicted minimum film thickness is a little nearer the pad centre than it actually is. This makes the cavitation zone larger, the pressure area smaller, and the minimum film thickness between 6 and 25 % too low (figure 5). The temperature is higher than it should be, which has been demonstrated in the last section. It will be seen how sensitive is this cycle of computation to small errors. It shows up very well any limitations in the basic assumptions in the theory. A fuller treatment would need to consider the variation of temperature *through* the film. Remarkably the maximum outlet temperature error is only 2.5 K.

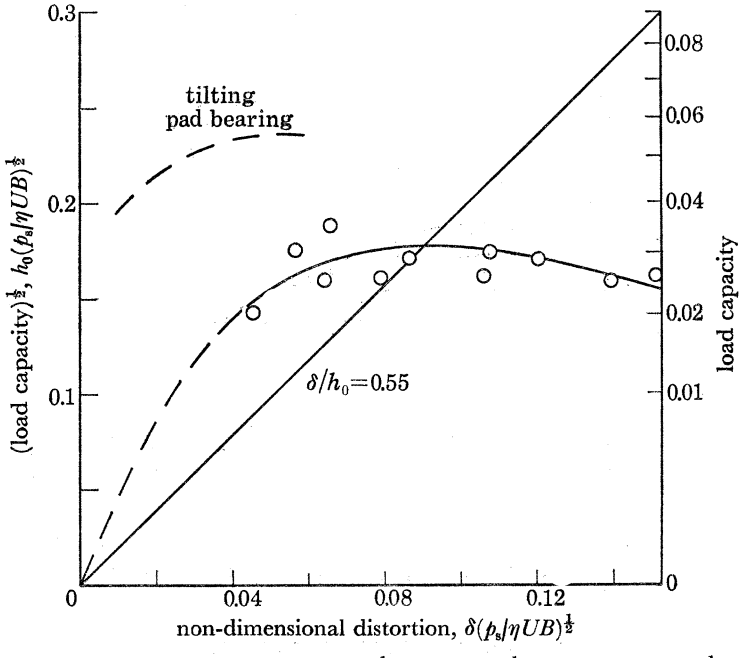

Figure 10. Plot of (load capacity)$^{\frac{1}{2}}$, $h_0(p_s/\eta UB)^{\frac{1}{2}}$ against $\delta(p_s/\eta UB)^{\frac{1}{2}}$.

The effect of distortion on load capacity

The square root of load capacity, $h_0(p_s/\eta UB)^{\frac{1}{2}}$, is plotted against non-dimensional distortion $\delta(p_s/\eta UB)^{\frac{1}{2}}$ in figure 10, together with the data obtained for the tilting pad bearing from part II, figure 17. It is surprising how constant the load capacity remains over a large range of distortion. This fits in well with Fogg's earlier results.

Load capacity appears to be a maximum when pad distortion is 0.55 times the minimum film thickness.

Comparison of tilting and parallel pad performance

In this series of tests there were six pads compared with three for the tilting pad bearing. Greater shear and churning, due to this and leading to greater heat generated, giving lower viscosities and hence smaller film thicknesses, makes a direct comparison difficult. Both parameters $h_0(p_s/\eta UB)^{\frac{1}{2}}$ and duty parameter $(\eta U/p_s B)^{\frac{1}{2}}$ take this viscosity effect into account. Plots of (load capacity)$^{\frac{1}{2}}$ against non-dimensional distortion (figure 10) and non-dimensional film

Downloaded from rsta.royalsocietypublishing.org

thickness (h_0/B) against duty parameter (figure 11) are used to compare performance of the different pads. The maximum load capacity for the parallel pad is 60 % of that for the tilting pad. Figure 11 shows that for high values of duty parameter, which corresponds to light conditions of lubrication, the tilting pad supports a 60 % thicker film than the parallel pad. As conditions for lubrication worsen, however, the minimum film thickness values converge so that at low values of duty parameter the advantage of the tilting pad reduces to 17 %.

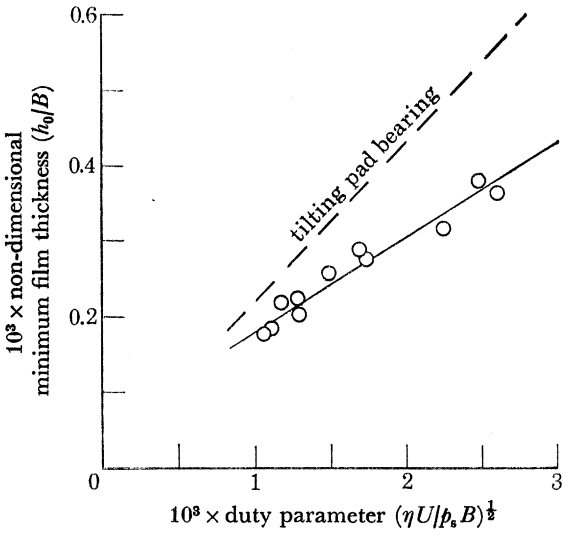

FIGURE 11. Plot of non-dimensional minimum film thickness (h_0/B) against duty parameter $(\eta U/p_e B)^{\frac{1}{2}}$.

CONCLUSIONS

It can be said that the interferometric technique has proved conclusively that the action of Beauchamp Tower's and of Fogg's 'parallel surface' bearings is due to thermal distortion as suggested by Swift and then by later workers. The extremely complete mapping of the film shape by interferometry enables this to be shown. Furthermore the analytical procedure gives a reasonable fit with measurements but the assumptions (all concerned with temperature) are stretched rather severely.

We would like to thank the Glacier Metal Co. for financial support for one of us and for supplying the test bearings.

REFERENCES

Cameron, A. 1960 *Engineering* **190**, 904.
Cameron, A. 1966 In *Principles of lubrication*, chs 5, 11. London: Longmans.
Cameron, A. & Wood, W. L. 1946 VIth Int. Congress Appl. Mech. In *Trans A.S.L.E.* **1**, 254 (1959).
Dowson, D. & Hudson, J. D. 1963 *Lub. Wear. Conv., Inst. Mech. Engrs*, p. 42.
Ettles, C. M. & Cameron, A. 1963 *Lub. Wear. Conv.*, paper no. 17.
Ettles, C. M. & Cameron, A. 1966 *Lub. Wear. Conv., Inst. Mech. Engrs.*
Fogg, A. 1946 *Proc. Inst. mech. Engrs.* **155**, 49.
Hemingway, E. W. 1965 *Proc. Inst. Mech. Engrs* **180**, part 1, no. 44.
Neal, P. B. 1963 *Lub. Wear. Conv., Inst. Mech. Engrs*, p. 49.
Osborne, M. R. 1966 In *Principles of lubrication*, ch. 18. London: Longmans.
Osterle, F., Charnes, A. & Saibel, E. 1953 *Trans A.S.M.E.* **75**, 1113.

PHILOSOPHICAL TRANSACTIONS OF THE ROYAL SOCIETY A MATHEMATICAL, PHYSICAL & ENGINEERING SCIENCES
PHILOSOPHICAL TRANSACTIONS OF THE ROYAL SOCIETY A MATHEMATICAL, PHYSICAL & ENGINEERING SCIENCES

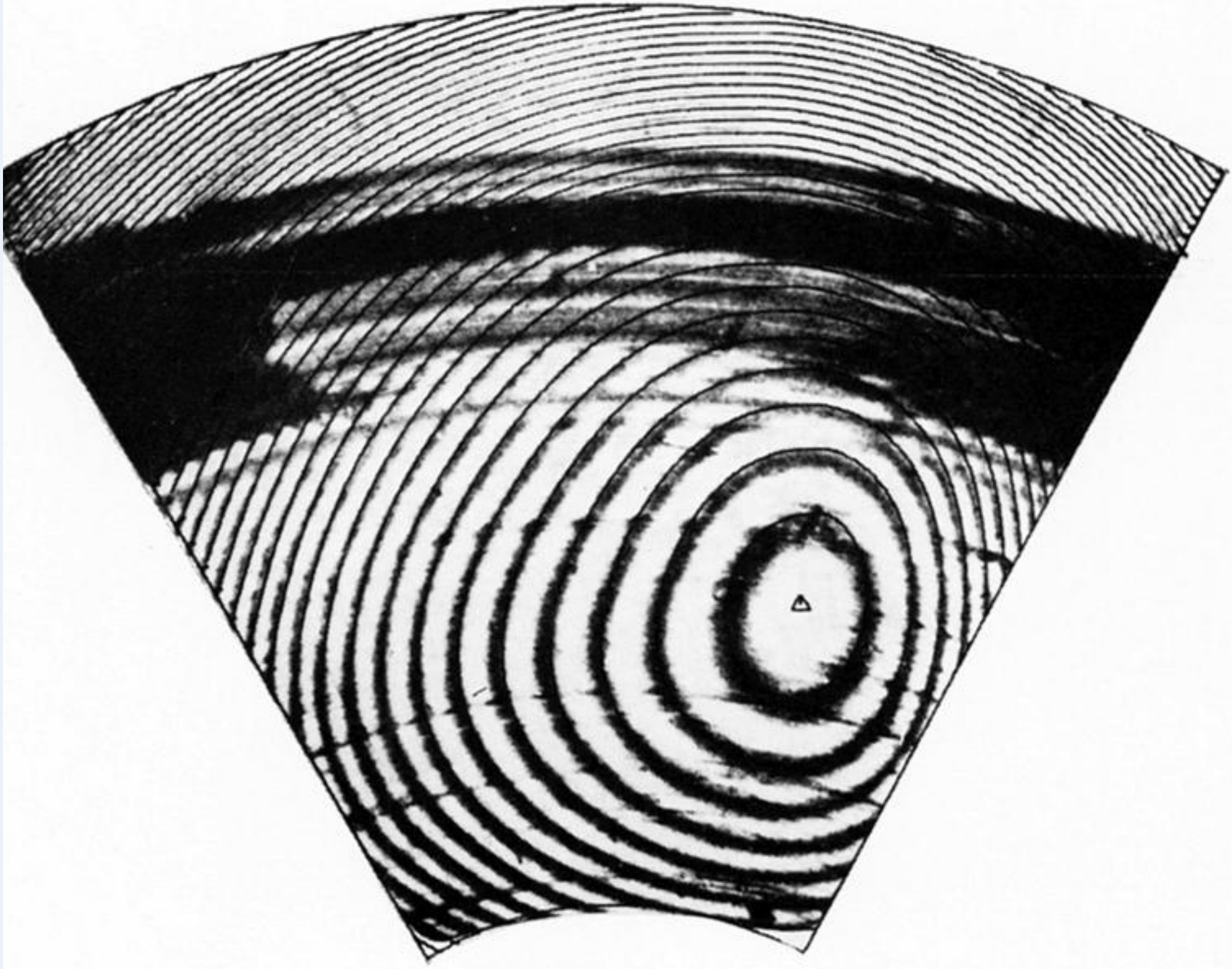

FIGURE 2. Typical interferogram with digital print out superimposed.

PHILOSOPHICAL TRANSACTIONS OF THE ROYAL SOCIETY A MATHEMATICAL, PHYSICAL & ENGINEERING SCIENCES
PHILOSOPHICAL TRANSACTIONS OF THE ROYAL SOCIETY A MATHEMATICAL, PHYSICAL & ENGINEERING SCIENCES

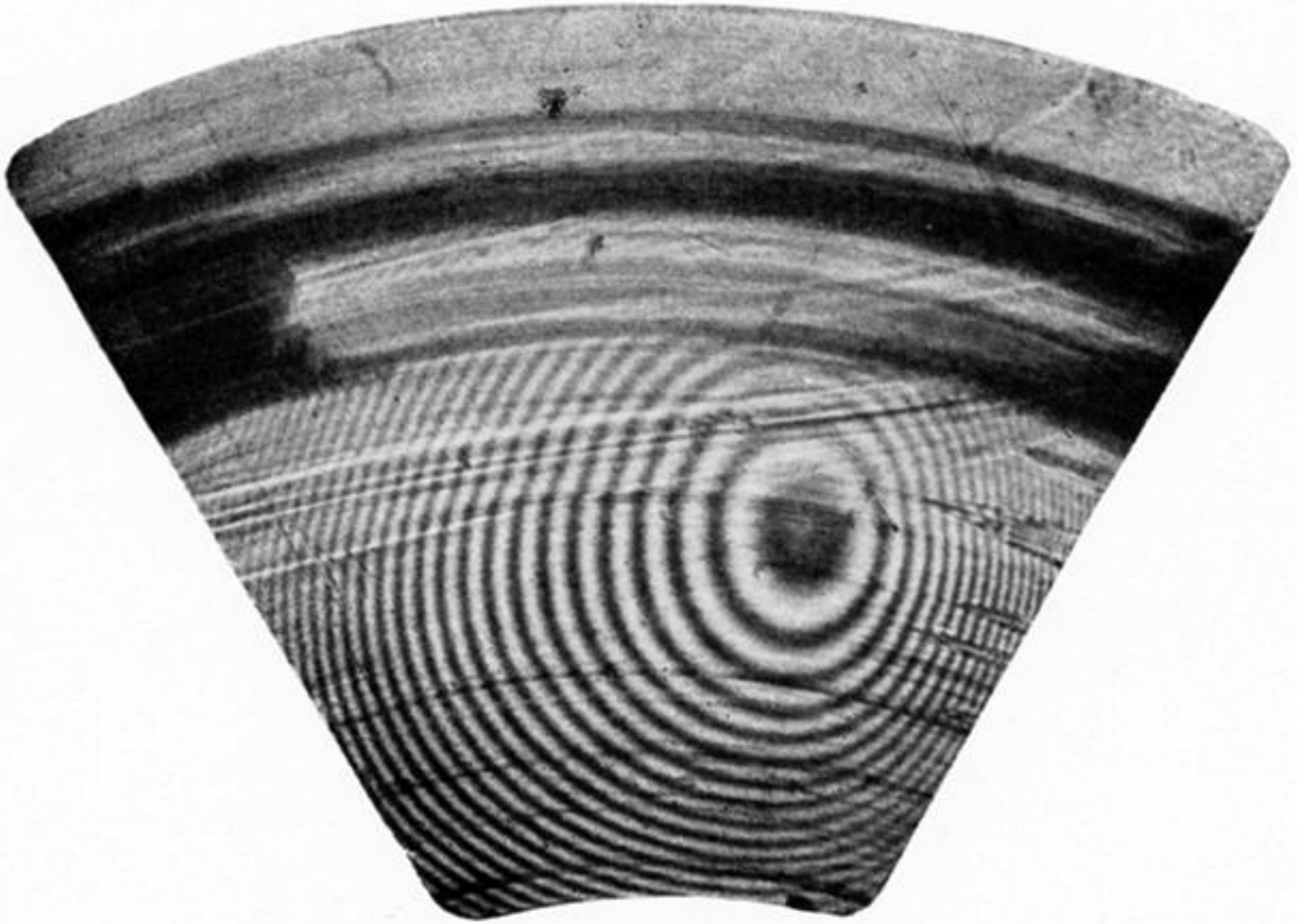

FIGURE 4. Interferogram of pad load 2.76 M/Nm², speed 582 rad/s showing film rupture.

PHILOSOPHICAL TRANSACTIONS OF THE ROYAL SOCIETY A MATHEMATICAL, PHYSICAL & ENGINEERING SCIENCES